ELSEVIER

Catalysis Today 56 (2000) 275–282

CATALYSIS TODAY

www.elsevier.com/locate/cattod

Simulation and experimental study on the polymer membrane reactors for the vapor-phase MTBE (methyl tert-butyl ether) decomposition

Jun Seon Choi [a], In Kyu Song [b], Wha Young Lee [a,*]

[a] *Department of Chemical Engineering, Seoul National University, Shinlim-dong, Kwanak-ku, Seoul 151-742, South Korea*
[b] *Department of Industrial Chemistry, Kangnung National University, Kangnung, Kangwondo 210-702, South Korea*

Abstract

Simulation and experimental studies on the polymer membrane reactor were examined for the vapor-phase MTBE (methyl tert-butyl ether) decomposition. A double pipe (shell and tube type) membrane reactor comprising 12-tungstophosphoricacid catalyst and polymer membrane was designed. The polymer membrane was coated on the porous alumina tube. Polyphenylene oxide (PPO), polysulfone (PSF) or cellulose acetate (CA) was used as a constituent membrane material. It was observed that permeabilities of methanol through each polymer membrane were higher than those of isobutene and MTBE regardless of the kind of polymer membrane used. The selective permeation of methanol through each polymer membrane shifted the chemical equilibrium toward the favorable direction in the MTBE decomposition reaction. MTBE conversions in the membrane reactors were much enhanced compared to the equilibrium conversions. The MTBE conversions were increased with the increase of reaction temperature and with the decrease of reaction pressure. Simulated results were in good agreement with the experimental results. The PPO membrane reactor showed the best performance in the experimental condition.

Keywords: MTBE; Membrane reactor; Heteropolyacid; Polymer membrane; Simulation

1. Introduction

A membrane reactor is a unit which consists of a membrane and a reactor. The membrane reactor has been spotlighted because of its simultaneous function of chemical reaction and separation. The total reaction conversion in the membrane reactor can be improved remarkably for the equilibrium limited reversible reactions by removing reaction products continuously from the reactor through a membrane. Therefore, the membrane reactor has many advantages over the conventional chemical reactors [1–3].

An inert membrane reactor is composed of a catalyst on the feed side and a membrane. The major investigations on the inert membrane reactor have been concentrated on the inorganic membrane reactors because of their excellent thermal stability at high reaction temperatures [4–7]. Although the applications of inorganic membrane reactors have been restricted on the reactions concerned with small molecules or decomposition reactions such as dehydrogenation reactions [8–10], polymer membrane reactors are more applicable than inorganic membrane reactors because polymer membranes have versatile diffusivity and solubility [11]. However, only a few works on the polymer membrane reactors have been reported [12–14]. It is generally believed that the gas permeability through a polymer membrane depends on interactions between poly-

* Corresponding author. Tel.: +82-2-880-7404; fax: +82-2-888-7295.
E-mail address: wyl@plaza.snu.ac.kr (W.Y. Lee).

0920-5861/00/$ – see front matter
PII: S0920-5861(99)00285-0

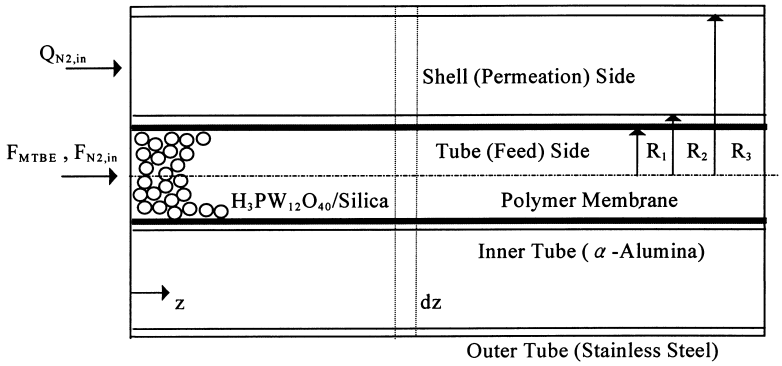

Fig. 1. Detailed structure of the double pipe (shell and tube type) polymer membrane reactor.

mer material and gas molecule. And the interaction is in turn affected by polymer properties such as structure, polarity, hydrogen bond, binding energy, density, chain property, chain mobility and pore characteristics. Therefore, it is difficult to quantify an individual effect of polymer properties on the gas permeability.

In this work, experimental studies on the reactor performance of the inert polymer membrane reactor were carried out and compared with simulation results which was developed on the basis of solution-diffusion model. A double pipe (shell and tube type) membrane reactor comprising heteropolyacid and polymer membrane was designed for the vapor-phase MTBE decomposition. 12-Tungstophosphoricacid ($H_3PW_{12}O_{40}$) supported on silica was used as an active catalyst for the reaction. Polyphenylene oxide (PPO), polysulfone (PSF) or cellulose acetate (CA) was used as a constituent membrane material for the membrane reactor.

A heteropolyacid (HPA) has acidic and redox catalytic properties at the same time. It also shows characteristic adsorption behaviors depending on the properties of adsorbates [15–18]. It is well known that HPA is an active catalyst for the MTBE synthesis and decomposition [19]. Although MTBE synthesis is an important chemical process, MTBE decomposition is also an attractive chemical process due to the potential demand for pure isobutene. It is know that MTBE synthesis and decomposition are a reversible and acid-catalyzed reaction [20–24].One mole of MTBE decomposes into equimolar amounts of methanol and isobutene.

2. Experimental and simulation

2.1. Materials

12-Tungstophosphoricacid ($H_3PW_{12}O_{40}$ from Aldrich Chem.) was used as an active catalyst for the vapor-phase MTBE decomposition. $H_3PW_{12}O_{40}$ (denoted as PW) was supported on silica (average particle size: 500–1000 μm, pore volume: 1.15 cm^3/g) by an incipient wetness method [25]. Final composition of the supported catalyst was 6 wt.% PW/silica. PSF (Udel 1700 from Union Carbide), PPO (poly-2,6-dimethyl-1,4-phenylene oxide from Aldrich Chem.) or CA (from Eastman Kodak) was used as a membrane material. Chloroform was used as a solvent for PSF and PPO while acetone was used as a solvent for CA. A porous double-layered alumina tube (α-Al_2O_3 from Dongsuh Ind., I.D.: 0.74 cm, O.D.: 1.0 cm, inside average pore size: 0.02 μm, outside average pore size: 13 μm) was used as an inorganic support for polymer membrane.

2.2. Design of polymer membrane reactor

Fig. 1 shows the details of the designed polymer membrane reactor. Three polymer membrane reactors were examined with the variation of polymer material. The porous alumina tube was used as an inner tube of the membrane reactor. A homogeneous solution of PPO (17 wt.%)–chloroform (83 wt.%) was coated on the tube (feed) side of the alumina tube, and subsequently it was dried at 100°C. PSF (17 wt.%)–chloroform (83 wt.%) solution or CA

(20 wt.%)–acetone (80 wt.%) solution was also coated on the tube side of the alumina tube to form a corresponding membrane reactor. The coated amount of polymer membrane was in the range from 0.45 to 0.5 wt.% polymer/alumina. The effective length of the reactor zone was in the range from 4.0 to 4.5 cm. All the end parts of the alumina tube were sealed with epoxy resin. A stainless steel tube (O.D.: 2.54 cm) was used as an outer shell of the membrane reactor. PW catalyst supported on silica was packed in the tube side for the reaction. No leakage was confirmed before the reaction.

2.3. Reaction and permeability

MTBE was sufficiently vaporized and fed to the membrane reactor continuously together with N_2 carrier ($Y_{N2} = 0.9$). Contact time (W/F_{MTBE}) was varied by controlling the amounts of MTBE feed within the range from 0.001 to 0.025 MTBE-mol/h. The reactor performance was examined at the reaction temperature of 80, 90 and 100°C. The performance of the individual membrane reactor was also examined at the pressure ranging from 1.0 to 2.3 atm. The permeated stream was continuously removed by N_2 sweeping gas (4.0 cm^3/min). The permeated and reacted (rejected) stream were periodically sampled and analyzed with a GC (Yanaco G180).

MTBE conversion and isobutene selectivity in the feed (tube) side were calculated as follows:

$$\text{MTBE conversion (\%)} = [1 - (\text{MTBE}_{\text{tout}} + \text{MTBE}_{\text{sout}})/\text{MTBE}_{\in}] \times 100,$$

$$\text{Isobutene selectivity in the feed(tube) side) (\%)} = I_{\text{out}}/[I_{\text{out}} + M_{\text{out}}] \times 100,$$

where MTBE_{in} is the amounts of MTBE in the feed flow, $\text{MTBE}_{\text{tout}}$ the amounts of MTBE in the effluent flow of the tube side, $\text{MTBE}_{\text{sout}}$ the amounts of MTBE in the effluent flow of the permeation (shell) side, I_{out} the amounts of isobutene in the effluent flow of the tube side, M_{out} the amounts of methanol in the effluent flow of the tube side.

Permeabilities of the reaction components through each polymer membrane coated on alumina tube were also measured at the temperature of 80, 90 and 100°C. The permeabilities were expressed as the gas permeation unit (GPU: 10^{-6} cm^3/cm^2 s cm Hg) instead of the permeability coefficient (cm^3 cm/cm^2 s cm Hg) because, the coating thickness of the polymer membrane on porous alumina was not perfectly uniform throughout the tube.

2.4. Simulation of polymer membrane reactor

A set of differential equations was derived through material balance for each component.

$$\text{Tube side : outlet flow rate} - \text{inlet flow rate} + \text{permeation rate} + \text{reaction rate} = 0,$$

$$\text{Shell side : outlet flow rate} - \text{inlet flow rate} + \text{permeation rate} = 0.$$

Fortran programming and the fourth order Runge–Kutta–Verner routine were used to solve differential mass balance equations with the boundary conditions. Non-linear regression of permeabilities was established with the variation of temperature and pressure for the computer simulation. Performances of the polymer membrane reactors were simulated with the variation of temperature, pressure, contact time and reactor length. Experimental reactor performances of the polymer membrane reactors were compared with the simulation results.

3. Results and discussion

3.1. Permeabilities and perm-selectivities of reaction components

Fig. 2 shows the permeabilities of reaction components through each polymer membrane at 90°C. The total permeation amounts of reaction components through polymer membranes were in the following order: PPO > CA > PSF. Except for the permeability of MTBE through CA membrane, the permeability of individual component through each polymer membrane was decreased with the increase of partial pressure of the corresponding component. It is noteworthy that the permeability of methanol was much higher than that of isobutene or MTBE regardless of the kind of polymer membrane used. This indicates that the permeated stream is methanol-rich and the reacted (rejected)

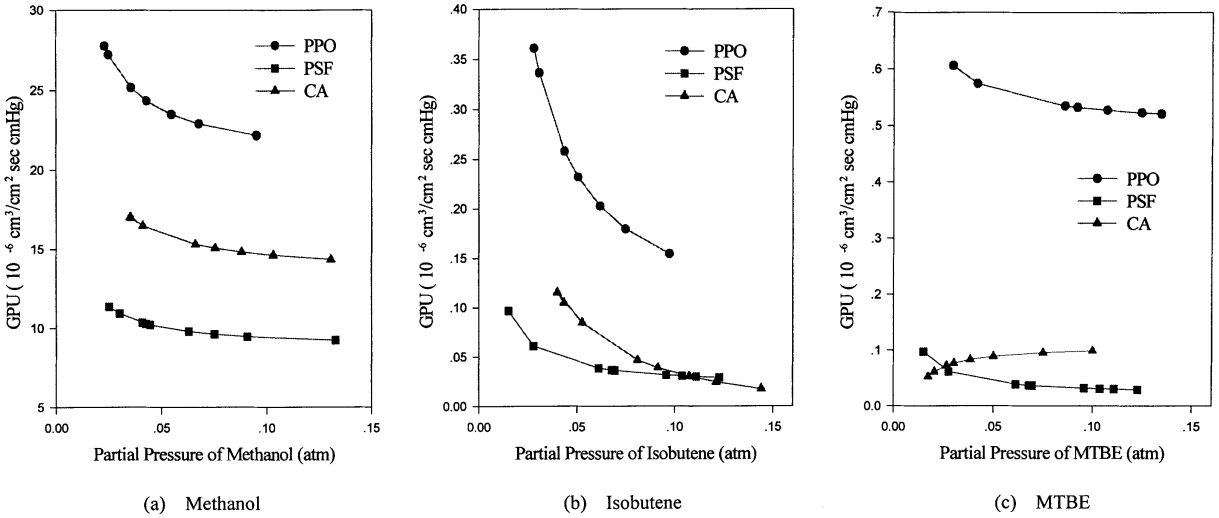

Fig. 2. Permeabilities of reaction components through each polymer membrane at 90°C with the variation of partial pressure.

stream is isobutene-rich flow. It also implies that the selective removal of methanol through each polymer membrane may shift the chemical equilibrium toward the favorable direction in the MTBE decomposition.

Fig. 3 shows the perm-selectivities of methanol/isobutene through each polymer membrane coated on alumina tube. The perm-selectivities of methanol/isobutene through each polymer membrane were increased at all temperatures with the increase of the partial pressure of MTBE. A direct comparison of the results in Fig. 3 also shows that the perm-selectivities of methanol/isobutene through PSF and CA membrane at a given partial pressure of MTBE were increased with the increase of temperature while that through PPO membrane at a given MTBE partial pressure showed the similar value with temperature. It

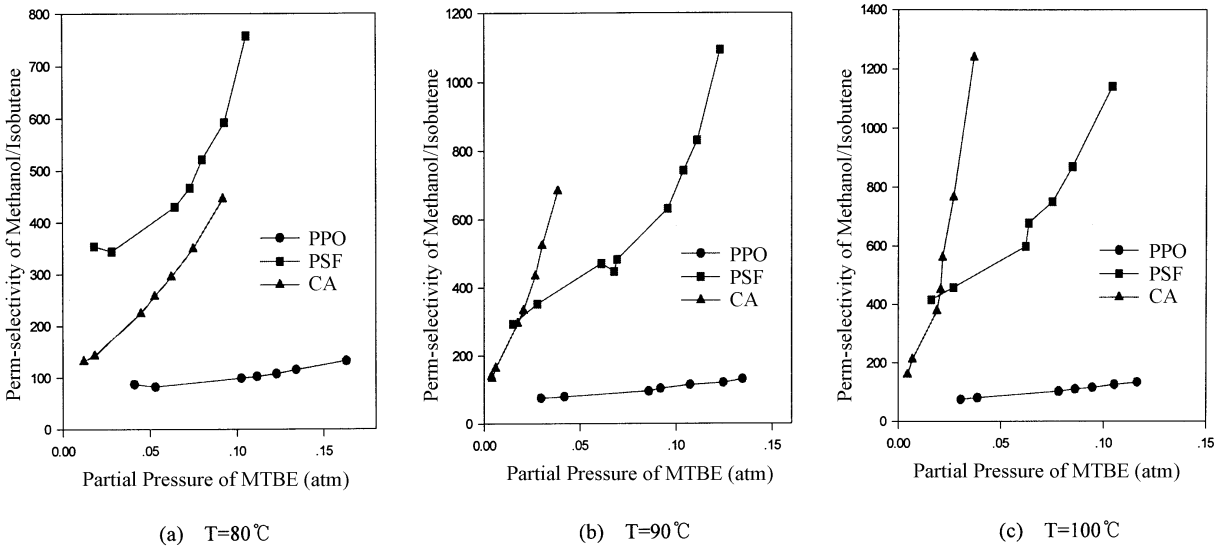

Fig. 3. Perm-selectivities of methanol/isobutene through each polymer membrane at various temperatures with the variation of partial pressure of MTBE.

Table 1
GPU (gas permeation unit) parameters for the non-linear regression of permeabilities

GPU = $a + b/P$ [atm]		Temperature (°C)					
		80		90		100	
		a	*b*	*a*	*b*	*a*	*b*
GPU (10^{-6} cm^3/cm^2 s cm Hg)							
PPO	MeOH	18.5	0.32	20.4	0.17	20.4	0.13
	Isobutene	0.090	0.006	0.071	0.008	0.056	0.010
	MTBE	0.483	0.003	0.496	0.003	0.465	0.001
PSF	MeOH	8.56	0.097	8.74	0.066	8.61	0.097
	Isobutene	0.002	0.001	0.002	0.001	−0.003	0.001
	MTBE	0.019	0.0005	0.020	0.001	0.017	0.0002
CA	MeOH	13.9	0.056	13.4	0.127	14.5	0.116
	Isobutene	−0.032	0.007	−0.02	0.005	0.006	0.005
	MTBE	0.133	−0.004	0.108	−0.001	0.137	−0.0004

was observed that PSF membrane showed the highest perm-selectivity of methanol/isobutene at 80°C while CA membrane showed the highest value at 100°C.

3.2. Comparison between simulation and experimental results

Runge–Kutta–Verner method was used for the simulation of the membrane reactor. The GPU parameters which were used for the non-linear regression of permeabilities were listed in Table 1.

Fig. 4 shows the typical simulation and experimental results for MTBE conversions at 2.3 atm and 80°C with the variation of W/F_{MTBE}. It is noteworthy that the simulation results were well matched with the experimental results. The MTBE conversions in all polymer membrane reactors were higher than the equilibrium conversions. This is because, the selective permeation of methanol through each polymer membrane shifted the chemical equilibrium toward the favorable direction. Fig. 5 shows the MTBE conversions and isobutene selectivities in the feed (tube) side of

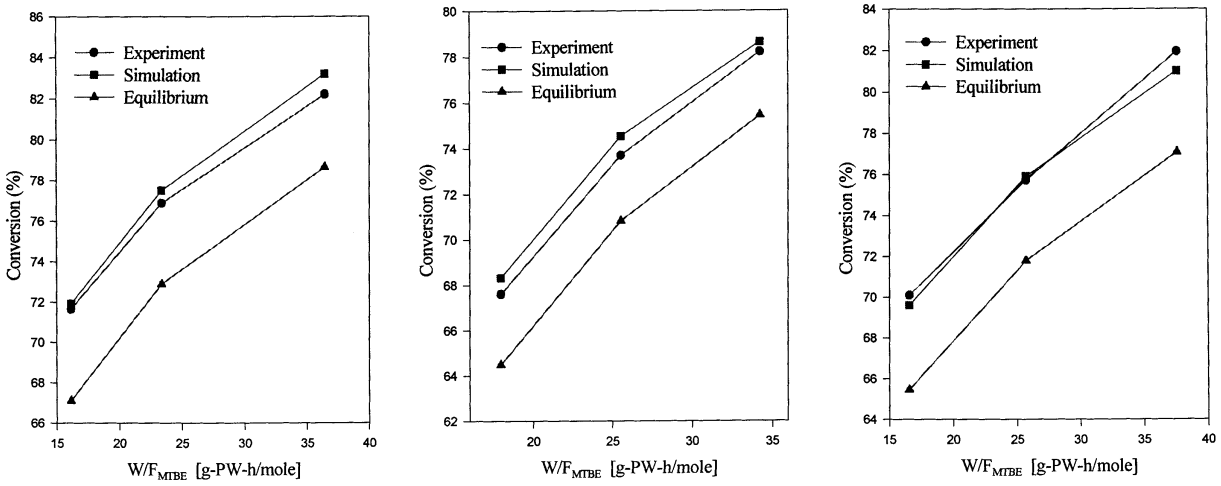

Fig. 4. Experimental and simulation results for the MTBE conversions at 2.3 atm and 80°C with the variation of W/F_{MTBE}.

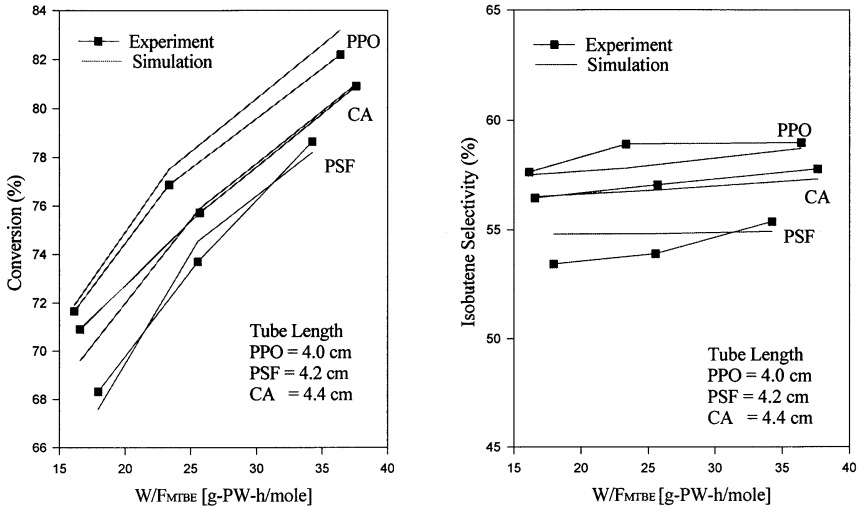

Fig. 5. MTBE conversions and isobutene selectivities in the feed (tube) side of the polymer membrane reactors at 2.3 atm and 80°C with the variation of W/F_{MTBE}.

the polymer membrane reactors at 2.3 atm and 80°C with the variation of W/F_{MTBE}. These results also clearly show that the simulation results were in good agreement with the experimental results within the error of ±5%. The performance of the membrane reactor at 2.3 atm and 80°C was in the following order: PPO > CA > PSF. This trend is in good agreement with the trend of isobutene selectivity in the feed (tube) side and with the trend of methanol selectivity in the permeation (shell) side in the following order: PPO > CA > PSF.

The effects of temperature and pressure on the MTBE conversions in the polymer membrane reactors were demonstrated in Figs. 6 and 7. The MTBE conversions were increased with the increase of reaction temperature and with the decrease of reaction pressure as expected from the thermodynamic equilibrium. The MTBE conversions were also increased

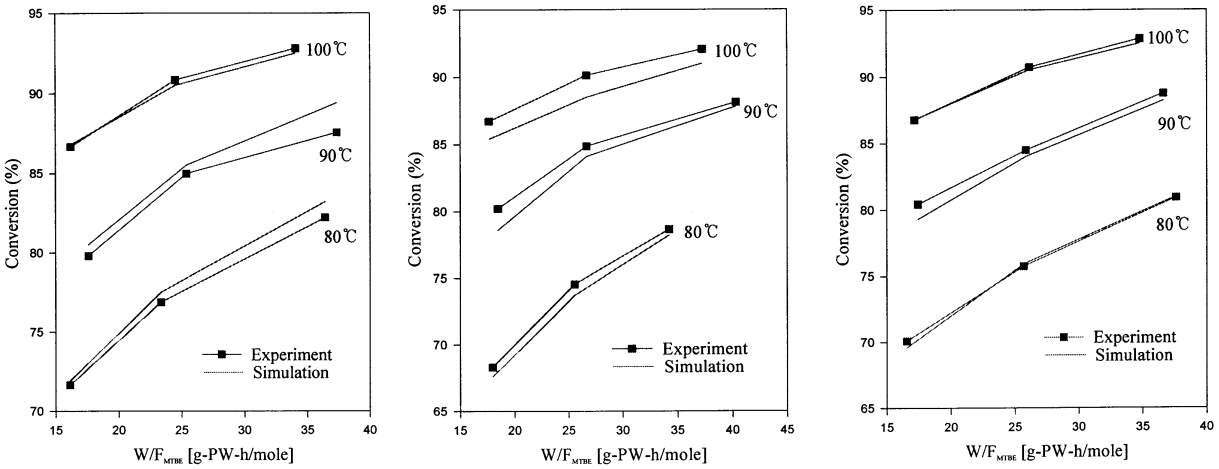

Fig. 6. Effects of temperature on the MTBE conversions in the polymer membrane reactors at 2.3 atm with the variation of W/F_{MTBE}.

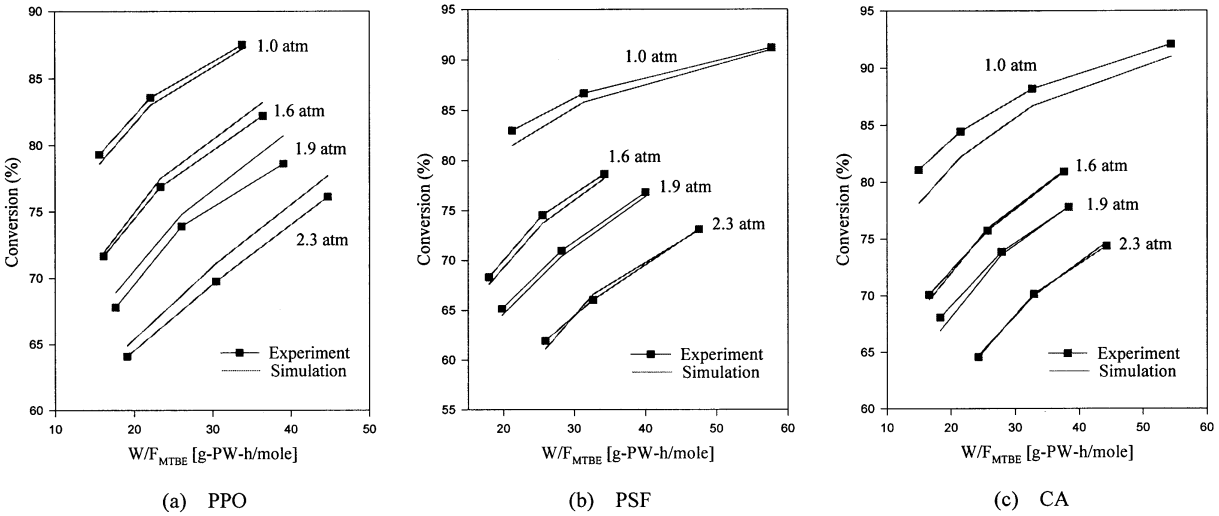

Fig. 7. Effects of pressure on the MTBE conversions in the polymer membrane reactors at 80°C with the variation of W/F_{MTBE}.

with the increase of contact time (W/F_{MTBE}). The simulation results were in good agreement with the experimental results with the variation of temperature and pressure. It is clear that the simulation program developed in this work can be used to describe the performance of the double pipe (shell and tube type) polymer membrane reactor for the vapor-phase MTBE decomposition. Only a non-linear regression for the permeability of reaction component through a newly equipped polymer membrane is required for the simulation of the new polymer membrane reactor.

3.3. Simulation of reactor performance along the reactor length

Fig. 8 shows the simulated profiles of MTBE conversions and isobutene selectivities in the feed (tube)

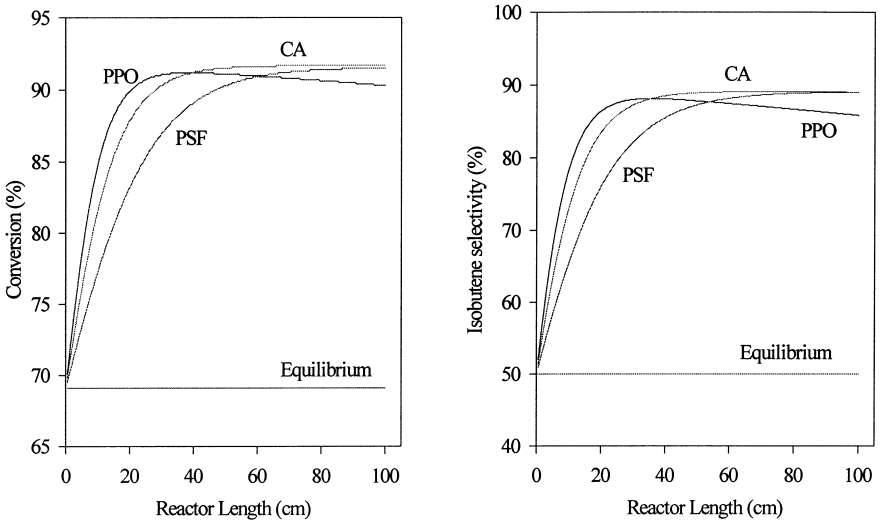

Fig. 8. Simulated profiles of the MTBE conversions and isobutene selectivities in the feed (tube) side along the reactor length at 1.6 atm and 100°C ($W/F_{MTBE} = 404.7$ g-PW-h/mol, $Y_{N2} = 0.5$).

side of the membrane reactors along the reactor length at 1.6 atm and 100°C. MTBE conversions and isobutene selectivities in CA and PSF membrane reactor were increased along the reactor length. However, PPO membrane reactor showed the maximum MTBE conversion and isobutene selectivity. The MTBE conversions and isobutene selectivities in each polymer membrane reactor showed the same trend. This means that the permeabilities of reaction products, methanol or isobutene, through polymer membrane strongly affect the equilibrium shift in this reversible reaction. The CA membrane reactor showed a better performance than PSF membrane reactor along the full range of reactor length simulated. The PPO membrane reactor showed the best performance within the reactor length of the experimental condition.

4. Conclusions

Simulation and experimental studies on the double pipe (shell and tube type) polymer membrane reactors were examined for the vapor-phase MTBE (methyl tert-butyl ether) decomposition. 12-Tungstophosphoricacid catalyst supported on silica was used as an active catalyst for the reaction. PPO, PSF or CA membrane coated on the porous alumina tube was used as a constituent membrane. It was observed that permeabilities of methanol through each polymer membrane were higher than those of isobutene and MTBE regardless of the kind of polymer membrane used. The selective removal of methanol through each polymer membrane shifted the chemical equilibrium toward the favorable direction in the model reaction. The perm-selectivities of methanol/isobutene through each polymer membrane were increased at all temperatures with the increase of the partial pressure of MTBE. MTBE conversions in the membrane reactors were much higher than the equilibrium conversions. The MTBE conversions were increased with the increase of reaction temperature and with the decrease of reaction pressure. The PPO membrane reactor showed the best performance in the experimental condition. Simulated results were in good agreement with the experimental results within the error of ±5%.

Acknowledgements

The authors wish to acknowledge the financial supports from Ilju Foundation and Daelim Industry for this work.

References

[1] S. Llias, R. Govind, AIChE Sympo. Ser. 85 (1989) 18.
[2] H.P. Hsieh, AIChE Sympo. Ser. 85 (1989) 53.
[3] M.P. Harold, P. Cini, B. Patenaude, AIChE Sympo. Ser. 85 (1989) 26.
[4] W.C. Pfefferle, US Pat. 3 290 496 (1966).
[5] T. Kameyama, Ind. Eng. Chem. Fundam. 20 (1981) 97.
[6] M. Stoukides, C.G. Vayenas, J. Catal. 70 (1980) 137.
[7] J.N. Michael, C.G. Vayenas, J. Catal. 85 (1984) 477.
[8] O. Shinji, M. Misono, Y. Yoneda, Bull. Chem. Soc. Jpn. 55 (1982) 2760.
[9] N. Itoh, Y. Shundo, K. Haraya, K. Obata, T. Hakuda, Int. J. Hydro. Ener. 9 (1984) 835.
[10] N. Itoh, AIChE J. 33 (1987) 1576.
[11] H.M. Madgavkar, Biotech. Bioeng. 18 (1977) 1719.
[12] J.K. Lee, I.K. Song, W.Y. Lee, Catal. Today 25 (1995) 345.
[13] J.K. Lee, I.K. Song, W.Y. Lee, Catal. Lett. 29 (1994) 241.
[14] I.K. Song, W.Y. Lee, J.J. Kim, Catal. Lett. 9 (1991) 339.
[15] M. Misono, Catal. Rev. -Sci. Eng. 29 (1987) 269.
[16] M. Misono, Mater. Chem. Phys. 17 (1987) 103.
[17] I.V. Kozhevnikov, Catal. Rev. -Sci. Eng. 37 (1995) 311.
[18] T. Okuhara, N. Mizuno, M. Misono, Adv. Catal. 41 (1996) 113.
[19] G.M. Maksimov, I.V. Kozhevnikov, React. Kinet. Katal. Lett. 39 (1987) 317.
[20] J. Tejero, F. Cunill, J.F. Izquierdo, Ind. Eng. Chem. Res. 280 (1989) 1269.
[21] F. Cunill, J. Tejero, J.F. Izquierdo, Appl. Catal. 34 (1987) 341.
[22] A. Rehfinger, U. Hoffmann, Chem. Eng. Sci. 46 (1990) 1605.
[23] A. Clementi, G. Oriani, F. Ancillotti, G. Poret, Hydrocarbon Proc. 59 (1979) 109.
[24] A. Convers, B. Juguin, B. Torck, Hydrocarbon Proc. 60 (1981) 95.
[25] C.N. Satterfield, Heterogeneous Catalysis in Practice, McGraw-Hill, New York, 1980, p. 68.